*Global Change Biology*

WILEY

Global Change Biology

RESEARCH ARTICLE

# Precipitation Pulse Dynamics Are Not Ubiquitous: A Global Meta-Analysis of Plant and Ecosystem Carbon- and Water-Related Pulse Responses

Emma Reich[1] | Jessica Guo[2] | Drew Peltier[3] | Emily Palmquist[4] | Kimberly Samuels-Crow[1] | Rohan Boone[1] | Kiona Ogle[1,5]

[1]School of Informatics, Computing, and Cyber Systems, Northern Arizona University, Flagstaff, Arizona, USA | [2]Hixon Center for Climate and the Environment, Biology, Harvey Mudd College, Claremont, California, USA | [3]School of Life Sciences, University of Nevada, Las Vegas, Nevada, USA | [4]U.S. Geological Survey, Southwest Biological Science Center, Flagstaff, Arizona, USA | [5]Department of Biological Sciences, Northern Arizona University, Flagstaff, Arizona, USA

**Correspondence:** Emma Reich (egr65@nau.edu)

**Received:** 26 November 2024 | **Revised:** 15 June 2025 | **Accepted:** 19 June 2025

**Funding:** This work was supported by National Science Foundation (NSF-EAR-1834699).

**Keywords:** Bayesian meta-analysis | coupled carbon-water cycle | drylands | precipitation intensification | precipitation pulse | pulse reserve

## ABSTRACT

Ecosystem responses to precipitation pulses ("pulse responses") exert a large control over global carbon, water, and energy cycles. However, it is unclear how the timing and magnitude of pulse responses will vary across ecosystems as precipitation regimes shift under accelerating climate change. To address this issue, this study evaluates how plants and ecosystems respond to precipitation pulses and explores potential implications of altered precipitation regimes for the carbon and water cycles. In particular, we conducted a global meta-analysis to quantify the magnitude and timing of plant and ecosystem carbon-related ($A_{net}$, NPP, GPP, $R_{eco}$, $R_{bg}$) and water-related (ET, T, $\Psi$, $g_s$) responses to 587 precipitation pulses. By analyzing pulse-response metrics published in the primary literature, we evaluated the characteristics of those pulse responses. We assessed whether precipitation pulses lead to a classic pulse response (i.e., a hump-shaped response as described by the pulse-reserve framework), a linear pulse response, a combination of classic and linear, or a lack of a pulse response. If a pulse response occurred, we explored the factors that drove its timing, magnitude, and speed. Our meta-analyses revealed that the classic, hump-shaped response is not ubiquitous, as it only accounted for 52% of the pulse responses. However, when a pulse response did occur, carbon-related responses to precipitation pulses were larger in magnitude (e.g., larger peak) than water-related pulse responses at relatively arid sites. However, at relatively mesic sites, this relationship reversed (i.e., water-related responses to precipitation pulses were larger than carbon-related responses). Additionally, larger precipitation pulse amounts increased water-related response magnitudes more than carbon-related response magnitudes across both arid and mesic sites. Therefore, under future precipitation intensification, carbon-related responses to precipitation pulses may become more decoupled from water-related pulse responses in wetter biomes but more coupled to water-related pulse responses in drier biomes.

Emma Reich and Jessica Guo contributed equally to this work. They should be considered as joint first authors.

## 1 | Introduction

Intensification of the global water cycle is leading to more infrequent and extreme precipitation events (Trenberth 2011; Pendergrass and Hartmann 2014; Pendergrass et al. 2017; Giorgi et al. 2019), superimposed upon longer and more persistent dry periods, enhanced vapor pressure deficits, and expanding aridification (Novick et al. 2016; Williams et al. 2022; Jacobson et al. 2024; Koppa et al. 2024). Ecosystem responses to precipitation events ("pulse responses") exert a large control over global carbon, water, and energy cycles (Kannenberg et al. 2020). The timing and frequency of rainfall events, then, may ultimately control whether ecosystems are carbon sinks or sources, especially in drylands (Delgado-Balbuena et al. 2023). Hence, quantification and attribution of carbon and water responses to precipitation pulses are critical to forecasting future ecosystem behavior.

The "pulse-reserve" framework describes how resource (e.g., precipitation) pulses are expected to influence various biological and abiotic responses (Noy-Meir 1973; Ogle and Reynolds 2004). In particular, the framework suggests that pulse responses are often nonlinear: an initial stimulatory response, followed by a delayed peak, and subsequent decline as the influence of the resource pulse passes (Noy-Meir 1973; Ogle and Reynolds 2004). Lagged responses to precipitation pulses (delayed peaks) can also occur and can vary from hours to days (Huxman, Smith, et al. 2004; López-Ballesteros et al. 2016). For example, some studies have found an initial and nearly immediate soil $CO_2$ efflux response when rainwater displaces accumulated $CO_2$ in shallow soil or due to rapid microbial oxidation of labile carbon substrates (Baldocchi et al. 2006; Matteucci et al. 2015; Scott and Biederman 2017). Others have found lagged effects of precipitation pulses on plant photosynthesis (Williams et al. 2009), likely due to leaf or annual plant growth in response to moisture pulses (Wohlfahrt et al. 2008). Components of carbon- and water-related pulse responses driven by microbial versus vegetation processes may thus exhibit differing lags (Garcia-Pichel and Sala 2022), challenging generalization across ecosystems.

Differing environmental conditions may affect the magnitude and timing of precipitation pulse responses across biomes. Classic hump-shaped or peaked responses described by pulse-reserve frameworks are more commonly observed in drylands (Ogle and Reynolds 2004; Reynolds et al. 2004; Collins et al. 2008, 2014) and are not as well documented in mesic systems with fewer sustained dry-down periods (Feldman et al. 2024). In mesic systems, pulse responses are less obvious, yet may still be driven by the frequency, amount, and timing of precipitation events (Feldman et al. 2021). Given higher soil water content and shorter intervals between events, pulse responses in mesic systems may not follow a classic, hump-shaped response. A framework capable of evaluating pulse responses across diverse ecosystems (or biomes) and pulse-response shapes is necessary to assess the generality of pulse dynamics in the face of global change (Santos e Silva et al. 2024; Koppa et al. 2024). This framework can help inform how global carbon and water cycles can shift under climate change, since individual precipitation pulse responses aggregate to influence large-scale carbon storage and regional water flux patterns.

While multi-site assessment of pulse responses is available from satellite remote sensing information (e.g., Feldman et al. 2021), no systematic synthesis of empirical studies has been conducted, potentially due to comparability issues that arise when integrating published results from across different studies (Vicca et al. 2012). For example, despite a long history of pulsed watering manipulations, differences in watering amount, timing, and post-pulse measurement frequency challenge direct intercomparison. To address this gap, we conducted a global meta-analysis of 41 published studies that describe the effect of precipitation pulses on ecosystem water and carbon responses across different scales, from leaves to ecosystems. For water-related responses, we focused on plant water potential ($\Psi$), stomatal conductance ($g_s$), transpiration (T), and evapotranspiration (ET). For carbon-related responses, we focused on leaf-level net photosynthesis ($A_{net}$), net primary productivity (NPP), gross primary productivity (GPP), ecosystem respiration ($R_{eco}$), and belowground respiration ($R_{bg}$). Using data summaries (published results) extracted for 587 water-related and carbon-related pulse responses across five biome types, we ask: (Q1) When do precipitation pulses lead to a classic pulse response (i.e., hump-shaped response as described by the pulse-reserve framework)? (Q2) When a pulse response occurs, what drives its timing, magnitude, and speed? And, (Q3) when a pulse response occurs, how does site aridity affect the pulse response?

We addressed these questions by applying Bayesian mixture models to literature-extracted data that account for experiment- and study-level effects, thus allowing us to estimate the magnitude of the pulse response (peak), timing of the peak, and speed and shape of the response (e.g., whether the response was classically hump-shaped, linear, or in-between) for multiple response variables. Then, we summarized the results from the Bayesian mixture models and used generalized linear models (GLMs) to evaluate the relationships between the estimated shape, magnitude, timing, and speed of the pulse response versus environmental and study conditions (e.g., pulse amount, site-level mean annual precipitation [MAP], site-level mean annual temperature [MAT], spatial scale of the observation, and whether the pulse response is carbon- or water-related). Synthesis of the Bayesian results via the GLMs provides insight into differences in pulse response dynamics across biomes and potential implications for the coupled carbon and water cycles.

## 2 | Methods

### 2.1 | Literature Search and Data Extraction

We conducted a literature search in Web of Science (data access time range: January 2019–March 2020) to identify studies that focused on the impacts of precipitation pulses on plant and ecosystem carbon and water response variables (i.e., $A_{net}$, NPP, GPP, $R_{eco}$, $R_{bg}$, ET, T, $\Psi$, $g_s$; refer to Table 1) across a range of ecosystem types (refer to Table 2 for search criteria/search

**TABLE 1** | List of precipitation pulse response variables targeted in this study.

| Variable type | Response variable | Description | Scale(s) of observation |
|---|---|---|---|
| Water-related | ET | Evapotranspiration | P |
| | T | Transpiration | L, I, P |
| | Ψ | Plant water potential | L, I, P |
| | $g_s$ | Stomatal conductance | L, I |
| Carbon-related | $A_{net}$ | Leaf photosynthesis | L, I |
| | NPP | Net primary productivity | L, I, P |
| | GPP | Gross primary productivity | L, P |
| | $R_{eco}$ | Ecosystem respiration | P |
| | $R_{bg}$ | Belowground respiration | P |

*Note:* The scale of observation reflects whether variables were measured or reported at the level of the leaf (L), individual plant (I), or plot/footprint (P). In the Bayesian models, all pulse responses are unitless and represented as the log-response ratio (LRR; Hedges et al. 1999) with respect to each response's value at time $t=0$ (immediately prior to pulse application).

**TABLE 2** | Summary of literature search terms and number of references found in Web of Science.

| Variable type | Search terms | Number of papers found | Number of papers used |
|---|---|---|---|
| Carbon-related | TOPIC: ((water* OR irrigation OR precipitation) AND (pulse OR addition) AND (experiment* OR manipulation) AND (photosyn* OR NEE OR respir* OR GPP OR GEE OR NPP OR NEP OR decomp*)) | 852 | 21 |
| Water-related | TOPIC: (precipitation AND *arid AND pulse AND evapotranspiration) | 65 | 8 |
| | TOPIC: (precipitation AND *arid AND pulse AND transpiration) | 61 | 7 |
| | TOPIC: (precipitation AND *arid AND pulse AND sap*) | 35 | 3 |
| | TOPIC: (precipitation AND *arid AND pulse AND evaporation) | 35 | 2 |

*Note:* All searches were refined to include English language literature only.

strings). We filtered our search results to only include studies that involved a water addition (e.g., natural precipitation event or artificial watering) that was temporally discrete, such that the water pulse was preceded by an extended rain-free period and no additional water was applied during the post-pulse study period. Published studies were also retained if they included: (1) pre-pulse measurements of the response variable, (2) measurements of the response variable over time, and (3) an adequate drying period before the next wetting event (if multiple pulse events occurred). The first literature search focused on carbon flux responses and was quite broad in its definition of "pulse." While this search yielded the most results (852 articles), only 1% of these papers included appropriate data as described above. Based on this experience, we targeted our water-related response searches to focus on individual response variables. Though this strategy yielded several duplicate papers, ~12% of the non-duplicate studies satisfied our criteria. In total, the complete literature search yielded 1048 studies for initial review, 41 papers retained, and data for 587 pulse responses (encompassing 225 separate pulse events or "pulse experiments" across five biomes; Figure 1).

Table 2 summarizes the results of the literature searches. These records represent nine different pulse response variables; 398 align with carbon-related variables and 189 with water-related variables. For most studies, multiple pulse response variables were recorded per pulse experiment event, e.g., a study may have recorded both GPP and ET after a single pulse application.

After identifying appropriate papers, we extracted pulse characteristics (e.g., including sample means and uncertainty estimates of the carbon- and water-related response variables of interest) and associated metadata from each paper. To extract sample means and uncertainty estimates, we used an R (R Core Team 2020) function ("digitize"; Poisot et al. 2016) and a MATLAB (The MathWorks Inc. 2020) function ("grabit.m"; Doke 2024). Where possible, we determined the location, MAP, MAT, and spatial scale of the study (Table 1), and whether the water pulse was experimental or natural. Not all studies included MAT and MAP, and missing values were extracted from WorldClim (Fick and Hijmans 2017) using site coordinates. While many studies occurred in semiarid and arid

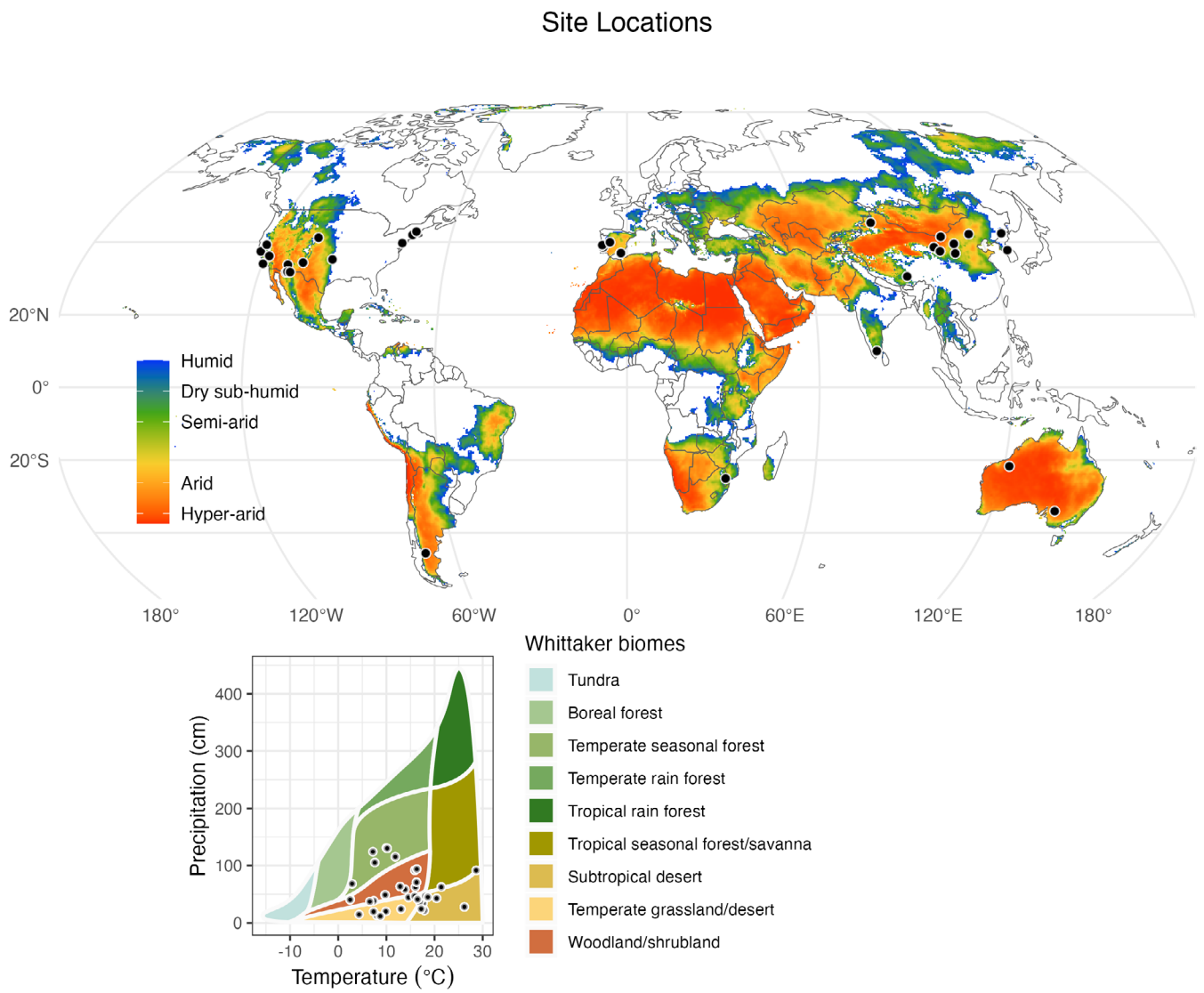


**FIGURE 1** | Map of study sites identified by the literature search. Although most sites occur in semiarid ecosystems in the northern hemisphere, our meta-analysis incorporated all studies that met our criteria (see Table 2), which included sites from five different biomes. Aridity data were calculated by taking the ratio of precipitation to evapotranspiration based on data obtained from the TerraClimate website. Transparent land areas indicate the aridity index was very humid (approaching infinity). Map lines delineate study areas and do not necessarily depict accepted national boundaries. Map of study sites identified by the literature search. Although most sites occur in semiarid ecosystems in the northern hemisphere, our meta-analysis incorporated all studies that met our criteria (see Table 2), which included sites from five different biomes. Aridity data were calculated by taking the ratio of precipitation to evapotranspiration based on data obtained from the TerraClimate website. Transparent land areas indicate the aridity index was very humid (approaching infinity). Map lines delineate study areas and do not necessarily depict accepted national boundaries.

biomes in the northern hemisphere, we extracted data from all studies that met our criteria, which included sites across five Whittaker biomes (figure 1, Ricklefs 2008), with MAP spanning 116–1311 mm.

We summarize our multi-step approach to synthesizing data extracted from the literature in Figure 2. Below, we first describe the specific mathematical models used to capture potential pulse response shapes, then we describe how we fit these models to the data within a hierarchical Bayesian meta-analysis framework. Finally, we summarize how we analyzed the output from the Bayesian meta-analyses to explicitly address our research questions.

## 2.2 | Synthesis and Modeling Approach

### 2.2.1 | Overview of Pulse-Response Models

Preliminary graphical analysis indicated some response variables exhibited the classic hump-shaped pulse response, others responded linearly, and some exhibited intermediate responses. Thus, we considered two functions for describing carbon- and water-related responses to precipitation pulses: a Ricker-inspired function (Bolker 2008) to capture classic, hump-shaped responses, and a simple linear function, where the response increases or decreases with time (Figure 2). We also considered a mixture of Ricker and linear functions, allowing for a diversity

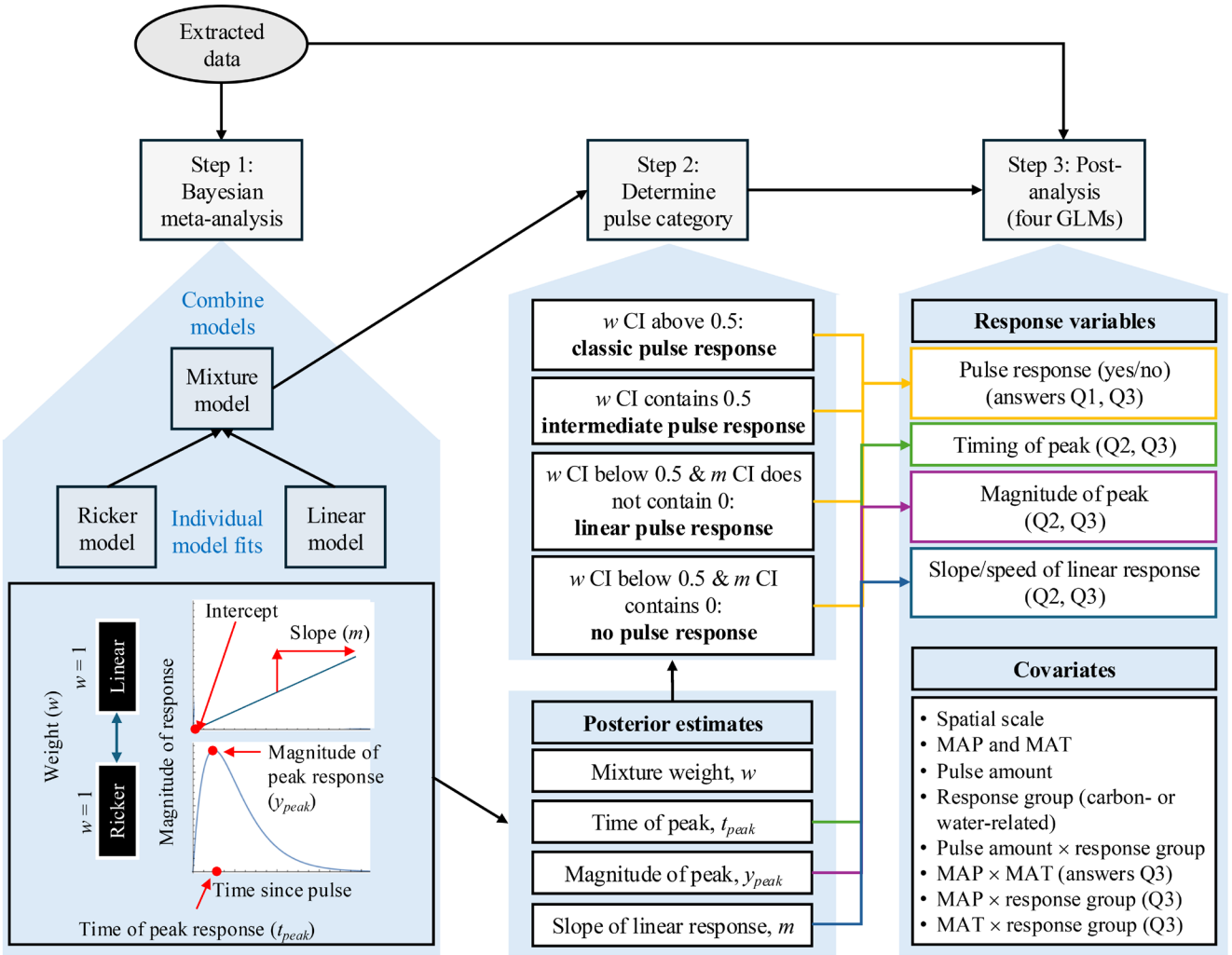


**FIGURE 2** | Flowchart summarizing our analysis framework, starting with extraction of information (data) from the literature, followed by three analysis steps. Step 1: Fitting the mixture model (focal model) and its individual model components (linear- and Ricker-only models) to the data, along with determining how to model the mixture weights (fixed [0 or 1] or treated as stochastic). Step 2: Using the parameter estimates from the mixture models to define the pulse type category for each pulse event. Step 3: Conducting generalized linear models (GLMs) to evaluate the factors influencing pulse response type and the pattern of the pulse response (shape, speed, magnitude). Here, *w* describes the relative contribution of the Ricker-type (hump-shaped) pulse response, whereas 1-*w* describes the relative contribution of the linear pulse response. The *w* CI is the credible interval for *w*, which was used to determine the pulse categories as described in *Determination of pulse response type*.Flowchart summarizing our analysis framework, starting with extraction of information (data) from the literature, followed by three analysis steps. Step 1: Fitting the mixture model (focal model) and its individual model components (linear- and Ricker-only models) to the data, along with determining how to model the mixture weights (fixed [0 or 1] or treated as stochastic). Step 2: Using the parameter estimates from the mixture models to define the pulse type category for each pulse event. Step 3: Conducting generalized linear models (GLMs) to evaluate the factors influencing pulse response type and the pattern of the pulse response (shape, speed, magnitude). Here, *w* describes the relative contribution of the Ricker-type (hump-shaped) pulse response, whereas 1-*w* describes the relative contribution of the linear pulse response. The *w* CI is the credible interval for *w*, which was used to determine the pulse categories as described in *Determination of pulse response type*.

of pulse response shapes that spanned a linear–Ricker gradient (Figure 3). Toward addressing Q1, we fit three models—Ricker-only, linear-only, or a mixture—to the extracted pulse response data. Here, we provide a general description of the three different functions.

The Ricker function describes how a response variable, *y*, varies with time since pulse application, *t*, given model parameters (*a* and *b*), such that $y(t, a, b) = a \cdot t \cdot e^{-b \cdot t}$. We reparametrized this model in terms of (1) the height of the peak response, $y_{\text{peak}}$ (e.g., the maximum value when the precipitation pulse stimulated the response or the minimum value when the precipitation pulse had in inhibitory effect or simulated a variable defined by negative values, such as for Ψ), and (2) the time at which this peak occurred, $t_{\text{peak}}$, with respect to $t = 0$ ($t = 0$ represents the time immediately before the water pulse was applied). Thus:

$$y(t, y_{\text{peak}}, t_{\text{peak}}) = y_{\text{peak}} e^{1 - \frac{t}{t_{\text{peak}}} + \log(t) - \log(t_{\text{peak}})} \quad (1)$$

The resulting model was also easier to fit compared to the original parameterization (refer to section *Implementation of Bayesian models*).

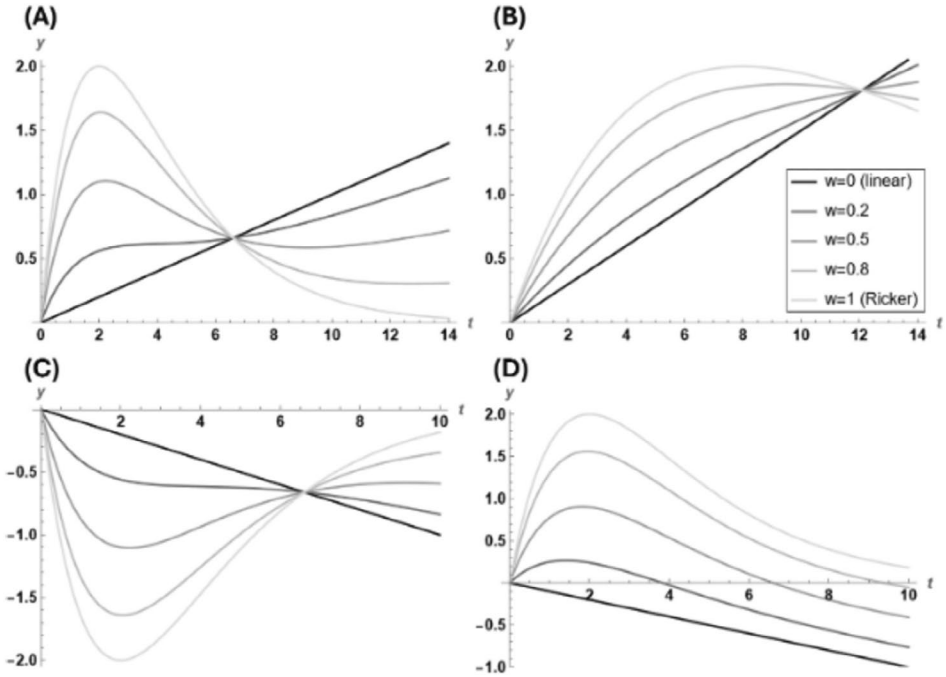


**FIGURE 3** | Example curves illustrating linear-only, Ricker-only, and mixtures of Ricker and linear functions. Examples are shown for mixture weights of $w=0$ (linear-only), $w=0.2$, $w=0.5$, $w=0.8$, and $w=1$ (Ricker-only). Parameter values representing different types of pulse responses are shown for (A) $b=0$, $m=0.1$, $t_{peak}=2$, $y_{peak}=2$, (B) $b=0$, $m=0.15$, $t_{peak}=8$, $y_{peak}=2$, (C) $b=0$, $m=-0.1$, $t_{peak}=2$, $y_{peak}=-2$, and (D) $b=0$, $m=-0.1$, $t_{peak}=2$, $y_{peak}=2$. When applied to the literature data, $t$ is time since application of the water pulse, and $y$ denotes the log-response ratio (LRR) for a given response variable of interest, where LRR is defined such that $y=0$ at $t=0$.

The linear function is simply given by:

$$y(t,b,m) = b + m \cdot t \tag{2}$$

where the intercept, $b$, describes the response variable, $y$, at time $t=0$, such that $b$ describes the value of $y$ immediately before a water or precipitation pulse. The slope, $m$, describes the "speed" of the linear response, or how quickly the response variable of interest reacts to the precipitation pulse.

The mixture model that combines (1) and (2) is given by:

$$y\left(t,y_{peak},t_{peak},b,m,w\right) = w \cdot y_{Ricker}\left(t,y_{peak},t_{peak}\right) + (1-w) \cdot y_{Linear}(t,b,m) \tag{3}$$

where $y_{Ricker}(t,\ y_{peak},\ t_{peak})$ and $y_{Linear}(t,\ b,\ m)$ are given by Equations (1) and (2), respectively; $w$ is the mixture weight that describes the relative contribution of the Ricker-type (hump-shaped) pulse response, whereas 1-$w$ describes the relative contribution of the linear pulse response. If $w=1$ (or $w=0$), then Equation (3) returns the Ricker (or linear) model; for $w$ between 0 and 1 (e.g., $w$ close to 0.5), Equation (3) describes a range of pulse responses characterized by a combination of hump-shaped and linear behavior (Figure 3).

### 2.2.2 | Bayesian Approach to Synthesizing Across Studies

To evaluate pulse response behavior, we computed the log-response ratio (LRR; Hedges et al. 1999) for each response variable with respect to its value at $t=0$. Thus, LRR = 0 just prior to the water pulse application ($t=0$). We assumed that the "observed" LRR values follow a normal distribution with a mean that is given by one of the above pulse response functions, either the Ricker, linear, or mixture model in Equations (1), (2), or (3), respectively. We specified hierarchical priors for the pulse experiment-level parameters ($y_{peak}$, $t_{peak}$, $b$, $m$, and $w$), centered on study-level parameters (again, often multiple pulse experiments were reported in a study). Finally, study-level parameters were assigned relatively non-informative priors. We provide details below.

We first implemented univariate models for each of the nine response variables. We used these models to inform the implementation of multivariate models that accounted for potential correlations among parameters associated with the response variables that were measured during the same pulse experiment (e.g., refer to Ogle et al. 2021). For both the univariate and multivariate models, we follow Ogle et al. (2021) and assume independent "measurement errors" such that the "observed" LRR values follow a normal distribution, such that for record $i$:

$$\text{LRR}_i \sim \text{Normal}\left(\mu_i, \sigma_i^2\right) \tag{4}$$

where $\sigma_i^2$ was calculated as the pooled variance using the standard deviations or standard errors for the associated response variable, as reported in the literature (as in Ogle et al. 2021). The mean, $\mu_i$, or expected LRR is given by one of the above pulse response functions, either the Ricker model in Equation (1), the linear model in Equation (2), or the mixture model in Equation (3).

For example, if using the mixture model:

$$\mu_i = y\left(t_i, y_{\text{peak}_{p(i),v(i)}}, t_{\text{peak}_{p(i),v(i)}}, b_{p(i),v(i)}, m_{p(i),v(i)}, w_{p(i),v(i)}\right) \quad (5)$$

where $t_i$ is the time (since pulse application) associated with record $i$, and $p(i)$ and $v(i)$ denote the specific pulse experiment, $p$, and response variable, $v$, associated with $i$. That is, the parameters (e.g., $y_{\text{peak}}$, ..., $w$) are allowed to vary by pulse experiment, $p$, and response variable, $v$.

In the univariate models, we specified univariate hierarchical priors for the pulse experiment-level parameters for each response variable, centered on study-level parameters, where $s(p)$ denotes study $s$ associated with pulse experiment $p$. Since the time at which the peak occurs should be after the pulse application (i.e., $t_{\text{peak}} > 0$), we assigned a prior on the log scale such that for $T_{\text{peak}} = \log(t_{\text{peak}})$:

$$T_{\text{peak}_{\text{p,v}}} \sim \text{Normal}\left(\sim T_{\text{peak}_{s(p),v}}, \sigma^2_{T_{\text{peak}_v}}\right) \quad (6)$$

We also truncated the prior at the maximum observed time since the pulse application for each pulse experiment so that $t_{\text{peak}}$ is not estimated to occur after the last measurement, thus helping to improve mixing, convergence, and interpretation of parameters in the Ricker model. We assigned hierarchical normal priors to the other pulse experiment-level parameters on their original scale without any truncation:

$$\begin{aligned} y_{\text{peak}_{p,v}} &\sim \text{Normal}\left(\sim y_{\text{peak}_{s(p),v}}, \sigma^2_{y_{\text{peak}_v}}\right) \\ b_{p,v} &\sim \text{Normal}\left(\sim b_{s(p),v}, \sigma^2_{b_v}\right) \\ m_{\text{p,v}} &\sim \text{Normal}\left(\sim m_{\text{s(p),v}}, \sigma^2_{m_v}\right) \end{aligned} \quad (7)$$

Given that the mixture weight, $w$, is constrained between 0 and 1, we gave it a hierarchical prior following the beta distribution:

$$w_{\text{p,v}} \sim \text{Beta}\left(\alpha_{\text{s(p),v}}, \beta_{\text{s(p),v}}\right) \quad (8)$$

The expected, study-level mixture weight is given by:

$$\sim w_{\text{s,v}} = \frac{\alpha_{\text{s,v}}}{\alpha_{\text{s,v}} + \beta_{\text{s,v}}} \quad (9)$$

All study-level and variable-specific parameters were assigned relatively noninformative, diffuse priors such that $\sim T_{\text{peak}_{\text{s,v}}}$, $\sim y_{\text{peak}_{\text{s,v}}}$, $\sim b_{\text{s,v}}$, and $\sim m_{\text{s,v}}$ were assigned *Normal* (0,10,000) priors, where 10,000 is the prior variance, and $\alpha_{\text{s,v}}$ and $\beta_{\text{s,v}}$ were assigned *Uniform*(1100) priors. The standard deviations in the hierarchical priors, $\sigma^2_{T_{\text{peak}_v}}$, $\sigma_{y_{\text{peak}_v}}$, $\sigma_{b_v}$, and $\sigma_{m_v}$, were assigned *Uniform*(0,100) priors.

The multivariate models followed a very similar structure as the univariate models, except that the pulse experiment-level parameters describing the shape of the pulse response (refer to Equations (6) and (7)) were assigned hierarchical multivariate normal priors to account for potential correlations among these response parameters. That is, for pulse experiment $p$, define $\theta p$ as the vector of parameters for multiple ($Nv$) response variables, such that, for $y_{\text{peak}}$, $\theta_{\text{p}} = (y_{\text{peak}_{p,1}}, y_{\text{peak}_{p,2}}, \ldots, y_{\text{peak}_{\text{p,Nv}}})$. Then, we assigned a multivariate normal hierarchical prior such that:

$$\theta_{\text{p}} \sim \text{Normal}\left(\sim \theta_{\text{s(p)}}, \Sigma\right) \quad (10)$$

where $\sim\theta_{\text{s}}$ is a vector (length $Nv$) of study-level parameters (e.g., containing the $\sim y_{\text{peak}_{\text{s,v}}}$ values), and $\Sigma$ is the $Nv \times Nv$ covariance matrix that describes correlations among the pulse experiment-level parameters across different response variables. The covariance matrices were assigned standard, relatively noninformative priors (i.e., Wishart priors for the precision matrices or inverse covariance matrices). The above multivariate normal prior was applied to each vector of pulse-experiment-level $T_{\text{peak}}$, $y_{\text{peak}}$, $b$, and $m$ parameters ($T_{\text{peak}}$ was truncated as in the univariate models).

Finally, returning to Equation (4), we note that some studies (e.g., 10 of 41 studies) did not report standard deviations or standard errors, resulting in missing values for their associated pooled variance, $\sigma_i^2$, in Equation (4). Thus, we treated the $\sigma_i^2$ as a stochastic quantity, similar to LRR in Equation (4), and, following Ogle et al. (2021), we assumed that the corresponding precision, $\tau_i$ ($\sigma_i^2 = 1/\tau_i$) followed a gamma distribution:

$$\tau_i \sim \text{Gamma}\left(\alpha_{\text{v}(i)}, \beta_{\text{v}(i)}\right) \quad (11)$$

We assigned *Uniform*(0,100) priors to the variable-specific hyperparameters, $\alpha_{\text{v}}$ and $\beta_{\text{v}}$. Thus, when $\sigma_i^2$ was available (not missing), the reported value was used in Equation (4); when $\sigma_i^2$ was missing (not reported), the missing value was imputed by Equation (11). Note that $\alpha_{\text{v}}$ and $\beta_{\text{v}}$ are informed by the records for which $\sigma_i^2$ was available.

### 2.2.3 | Implementation of Bayesian Models

The univariate Ricker, linear, and mixture models were fit separately to each pulse response variable (i.e., $A_{\text{net}}$, NPP, GPP, $R_{\text{eco}}$, $R_{\text{bg}}$, ET, T, Ψ, and $g_{\text{s}}$ [Table 1]), for a total of 27 model implementations (3 models × 9 variables). We implemented each model in R (R Core Team 2020) using JAGS (Plummer 2003) via the "jagsUI" package (Kellner and Meredith 2024). JAGS employs Markov chain Monte Carlo (MCMC) methods to sample parameters from the posterior distribution, and we simulated three MCMC sequences. We used the potential scale reduction factor, $\hat{r}$ (Gelman and Rubin 1992; Brooks and Gelman 1998), provided in the jagsUI output, to check for convergence of each parameter; we assumed chains converged if $\hat{r} < 1.2$. Using the converged samples, jagsUI calculated posterior means and central 95% credible intervals (CI) for each parameter.

For most pulse experiments, the mixture weights, $w_{\text{p,v}}$, in the mixture model were allowed to vary stochastically according to the hierarchical prior in Equation (8). However, for some pulse experiments, their parameters exhibited poor mixing and convergence, likely due to weights approaching values close to 0 or 1. In these cases, we set the weight, $w_{\text{p,v}}$, to a fixed

value such that either the Ricker ($w_{p,v} = 1$) or linear ($w_{p,v} = 0$) function was only used. We employed a set of rules, based on convergence/mixing behavior of initial simulations with the univariate models, to determine how to model each $w_{p,v}$ for each pulse experiment, $p$, and each response variable, $v$. We then reran the univariate mixture models to obtain posterior estimates for all remaining stochastic parameters of interest (Appendix S1).

Finally, we ran the multivariate mixture models, using the rules for modeling the weights (stochastic or fixed at 0 or 1) based on the univariate models. We implemented two different multivariate models based on groups of variables that showed notable overlap across pulse experiments. That is, many pulse experiments simultaneously measured ecosystem-level fluxes (e.g., ET, NPP, GPP, and $R_{eco}$) or leaf-level responses (e.g., $A_{net}$, T, Ψ, and $g_s$). $R_{bg}$ was rarely measured with one or more of the other responses, and very few pulse experiments produced data on both ecosystem-level fluxes and leaf-level responses. Thus, we implemented two multivariate models, one for the ecosystem-level fluxes ($Nv = 4$) and one for the leaf-level responses ($Nv = 4$). We then ran the multivariate mixture models to obtain posterior estimates for all remaining stochastic parameters of interest, and we focus on the results from these models for subsequent inference and post-analysis (refer to the next section).

## 3 | Evaluating Bayesian Model Results

### 3.1 | Determination of Pulse Response Type

We used the posterior estimates for the pulse experiment-level mixture weight, $w_{p,v}$, obtained from the final mixture model fits—univariate model for $R_{bg}$ and the multivariate models for all other response variables—to qualitatively define the pulse response shape for each pulse experiment and each response variable. We identified four "categories" that best describe possible shapes of the pulse response (Figure 2). If the 2.5th percentile (lower CI value) for $w_{p,v}$ was above 0.5 (i.e., the response is more Ricker-like), we assigned the classic pulse response shape designation. If the 95% CI for $w_{p,v}$ overlapped 0.5 (i.e., the response is between Ricker and linear), we assigned the intermediate pulse response shape. If the 97.5th percentile (upper CI value) for $w_{p,v}$ was below 0.5 (i.e., the response is more linear) and the 95% CI for the slope, $m_{p,v}$, did not overlap 0, we assigned the linear pulse response shape. If the 97.5th percentile for $w_{p,v}$ was below 0.5 (i.e., the response is more linear) and $m_{p,v}$ was not significant (95% CI overlapped 0), we assigned the no pulse response designation.

### 3.2 | Post-Analysis and Explanation of Covariates

We answered our three main questions by conducting a post-analysis using the posterior parameter estimates from our final Bayesian models and the assigned pulse response type categories (Figure 2). Our post-analysis consisted of four generalized linear model (GLM) analyses (refer to Table 1 for covariates). We chose to use GLMs for all post-analyses for flexibility and consistency, as we could easily change the distribution depending on the focal dependent variable. Our covariates included response group (i.e., carbon- or water-related response variable), spatial scale (i.e., leaf, individual, or plot/footprint; Table 1), MAT (mean annual temperature), MAP (mean annual precipitation), pulse type (i.e., natural or experimentally applied), and pulse amount. We also included an interaction of pulse amount × variable group to better understand how changes in pulse amount could uniquely affect carbon- and water-related responses. Note that although we group pulse response variables into carbon- or water-related groupings in the post-analysis, the original Bayesian models did not impose these groups and were applied to all nine response variables (i.e., ET, T, Ψ, and $g_s$, $A_{net}$, NPP, GPP, $R_{eco}$, $R_{bg}$; Table 1). Although these response groups are a simplification and include responses that are biologically very different, grouping pulse response variables into carbon- and water-related groups in the post-analysis can lend insight into how different components of the coupled carbon-water cycles may be impacted by changes in future precipitation regimes.

To address our first question (Q1)—When do precipitation pulses lead to a classic pulse response?—we used a GLM to model a binary dependent variable, where "classic", "intermediate", and "linear" pulse response indicated a response to the pulse and "did not respond to the pulse" was no response to the pulse. Pulse response (yes/no) was thus modeled as a function of the covariates: spatial scale (leaf, individual, plot/footprint), MAP, MAT, pulse amount, and response group (water- or carbon-related). We also included interactions between pulse amount × response group, MAP × response group, and MAP × MAT.

To address Q2—When a pulse response occurs, what drives its timing, magnitude, and speed?—We used the posterior means for the pulse experiment-level $y_{peak}$ as the dependent variable in a GLM to determine what drives the magnitude of the pulse response. We only considered absolute magnitude so that the direction of each response was aligned (e.g., traditionally, a more negative Ψ corresponds to a more hydrated xylem, but here we took the absolute value so it would be comparable with pulse responses such as ET). We conducted a separate GLM for $t_{peak}$ to determine what drives the timing of the pulse response. To determine what drives the speed of the peak response, we used the posterior mean of the slope, $m$, as the dependent variable in a third GLM. For all three GLMs, we used a Gaussian distribution for the $y_{peak}$, $t_{peak}$, and $m$ "response" values. For the first two GLMs for $y_{peak}$ and $t_{peak}$, we only focused on pulse experiments that were classified as showing a classic or intermediate pulse response; for the third GLM for $m$, we focused on pulse experiments classified as showing a linear or intermediate pulse response.

To address Q3—When a pulse response occurs, how does site aridity affect the pulse response?—we included two interactive effects in all GLMs: MAP × MAT and MAP × response group to evaluate how the pulse response behavior differs across ecosystems varying in their aridity (as captured by differences in MAP and MAT), and how the responses of carbon- versus water-related variables might be modulated by general ecosystem moisture status (MAP). To help interpret these interaction effects, we used the R package "interactions" (Long 2021) to generate interaction plots. Site MAT and MAP were uncorrelated ($r = -0.002$) across the studies we extracted

data from, and we were thus able to make inferences about the potential independent and interactive effects of site-level MAP and MAP.

## 4 | Results

### 4.1 | Bayesian Mixture Model Results

Based on the assessment of the mixture weights, $w_{p,v}$, and linear slopes, $m_{p,v}$, produced by the Bayesian mixture models, most (308) pulse responses were classified as classic, while 14 were classified as intermediate, and 120 as linear. The remaining 145 cases were identified as lacking a pulse response altogether (linear with a non-significant slope; Figure 4 and Figure S1).

Across all weights associated with each pulse response, 241 pulse experiment-level mixture weights aligned with a Ricker-type response ($w_{p,v}=1$; i.e., 100% Ricker), 265 with a linear response ($w_{p,v}=0$; i.e., 100% linear), and 81 were treated as stochastic with the potential to be a mixture of a Ricker- and linear-type response ($0<w_{p,v}<1$). Note that although many weights were determined stochastically, we still used the posterior means and CIs for the stochastic weights to group each pulse response as either classic, intermediate, or linear.

### 4.2 | Q1: When Do Precipitation Pulses Lead to a Classic Pulse Response?

Classic pulse responses accounted for more than half of the total responses. Among all pulse experiments, hump-shaped pulse responses were dominant for 245 of 398 (62%) carbon-related responses, but only 59 of 189 (31%) water-related responses. Classic pulse responses for carbon-related variables were most common at the plot/footprint level, while for water-related responses, classic responses were most common at the leaf level (Figure S1). GLM analyses showed that the likelihood of a pulse response occurring (or not occurring) was essentially independent of scale ($p>0.05$; Figure 5).

### 4.3 | Q2: When a Pulse Response Occurs, What Drives Its Timing, Magnitude, or Speed?

Broadly, pulse responses were slower at larger spatial scales and in hotter sites, though MAP and MAT also interacted to affect the speed of the response (Figure 6). Among the 322 classic or intermediate pulse responses, responses at large spatial scales (plot/footprint level) were faster and of smaller magnitude compared to leaf-level responses ($p<0.05$; Figure 5). Water-related pulse responses were more likely to have a smaller magnitude peak ($p<0.05$; Figure 5, negative effect of water-related responses on the magnitude of the peak). Hotter sites were associated with larger magnitude responses ($p<0.05$; Figure 5, positive effect of MAT on the magnitude of the peak). Among the 134 linear and intermediate pulse responses, wetter sites had faster response times ($p<0.05$; Figure 5, positive effects of MAP on the slope of the linear component of the response). Interestingly, larger water inputs had a significant, positive interaction with water- and carbon-related pulse responses ($p<0.05$; Figures 5 and 6, interaction between pulse amount and water- and carbon-related responses had a negative effect on the magnitude of the peak and linear speed), but pulse amount alone did not affect the magnitude or speed of the pulse response ($p>0.05$; Figure 5). The effect of pulse amount on the magnitude of the peak response varied among response-type groups, such that for water-related response variables, the magnitude of the peak was greater following large precipitation pulses relative to carbon-related responses (Figure 6A). Figure S2 shows the distribution of posterior means for $t_{peak}$, $y_{peak}$, and $m$ (linear slope) for all pulse responses.

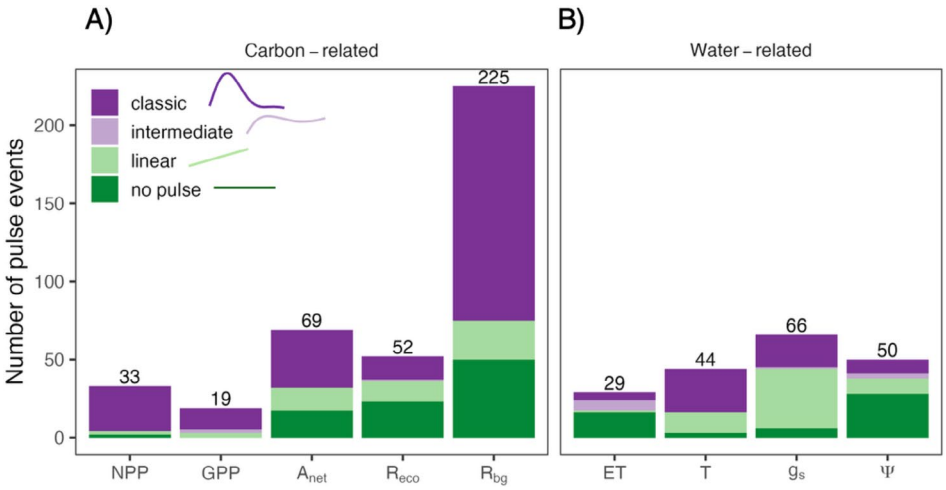


**FIGURE 4** | Number of pulse events (pulse experiments) extracted from the literature for (A) carbon-related and (B) water-related response variables that align with a classic, hump-shaped (Ricker-type; dark purple), intermediate (mixture of classic and linear; light purple), or linear (light green) pulse response, or that did not exhibit a pulse response (dark green). The carbon-related responses include net primary productivity (NPP), gross primary productivity (GPP), leaf-level net photosynthesis ($A_{net}$), ecosystem respiration ($R_{eco}$), and belowground respiration ($R_{bg}$); the water-related responses include evapotranspiration (ET), transpiration (T), stomatal conductance ($g_s$), and plant water potential (Ψ).

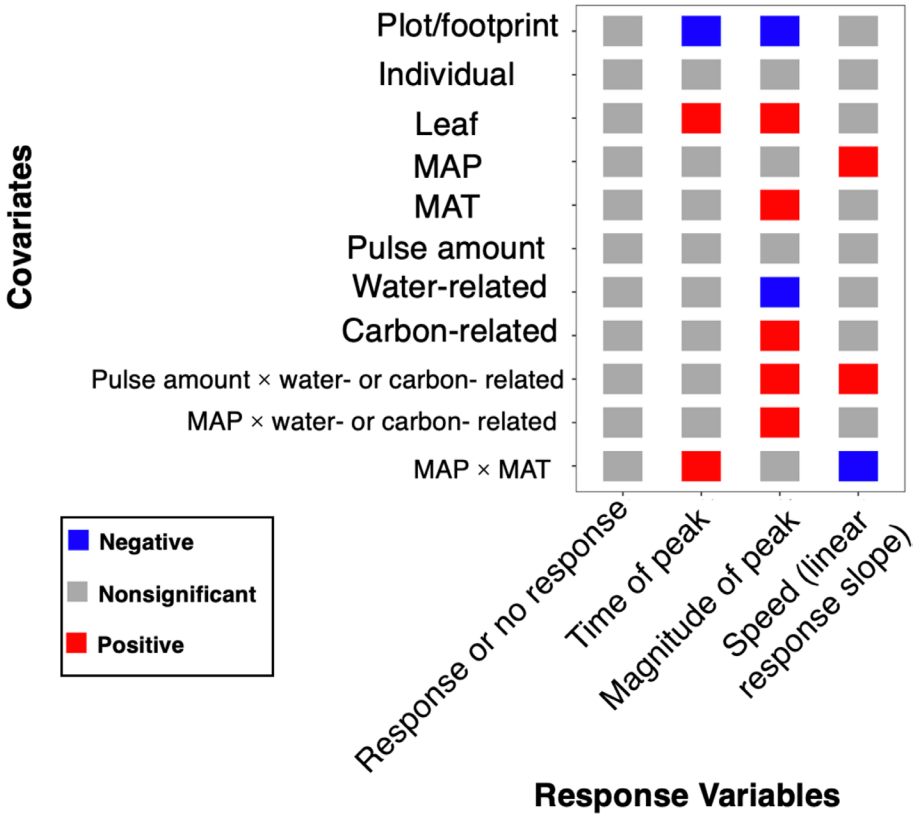


**FIGURE 5** | Results from four generalized linear models (GLMs) applied to the results obtained from the Bayesian meta-analysis final mixture models. Significantly ($p < 0.05$) positive effects are shown in red and significantly negative effects are shown in blue. The *y*-axis (rows) shows the different covariates included in each GLM and the *x*-axis (columns) shows the response variables used (i.e., variables that summarize components of the meta-analysis output and estimated pulse response characteristics). Categorical covariates (e.g., spatial scale, water- vs. carbon-related) were evaluated with respect to a reference level (i.e., leaf-level carbon-related responses).

### 4.4 | Q3: When a Pulse Response Occurs, How Does Site Aridity Affect the Pulse Response?

Relative to carbon-related variables, the responses of water-related variables to precipitation pulses were of larger magnitude at wetter sites and of smaller magnitude at drier sites (Figure 6B). We use MAP × MAT as a general index of aridity; this interaction was significant for the timing of the peak response (cold sites had faster times to peak relative to hot sites, but only at high levels of MAP; $p < 0.05$; Figure 5). Alone, higher MAT aligned with larger pulse responses, but there were no statistically significant main effects of MAP on the magnitude of the peak response (Figure 5). However, the MAP × response group interaction was significantly positive ($p < 0.05$) for the magnitude of the peak ($y_{peak}$; Figure 5). In particular, $y_{peak}$ of water-related pulse responses increased with increasing MAP, while $y_{peak}$ for carbon-related responses decreased with MAP (Figure 6B). Water- and carbon-related response variables also exhibit divergent relationships between the magnitude of their peak response ($y_{peak}$) and pulse amount, with $y_{peak}$ for water-related variables being strongly positively correlated with pulse amount, whereas $y_{peak}$ for carbon-related variables is only slightly positively correlated with pulse amount across the range of pulse amounts explored in this study (Figure 6A).

## 5 | Discussion

The results from our synthesis indicate that future intensification of precipitation pulse regimes is likely to uniquely affect carbon- and water-related responses across different ecosystem types and at different spatial scales. Our results show that classic (e.g., hump-shaped) pulse responses are not ubiquitous, even within arid and semiarid systems where classic pulse responses are expected to be most common. When notable pulse responses did occur, their timing and the magnitude of the peak response varied among carbon- and water-related response variables, which was further mediated by site characteristics and precipitation pulse amount. Below, we explore the implications of our results in the context of our three research questions.

### 5.1 | Q1: When Do Precipitation Pulses Lead to a Classic Pulse Response?

Previous studies have found that pulse responses are more easily observed in places with low MAP (Feldman et al. 2021), but are also present at sites with higher MAP, though less reflective of classical pulse dynamics. We found that pulse responses exist regardless of site MAP and MAT. Few studies have explored pulse dynamics in mesic ecosystems, likely due to the

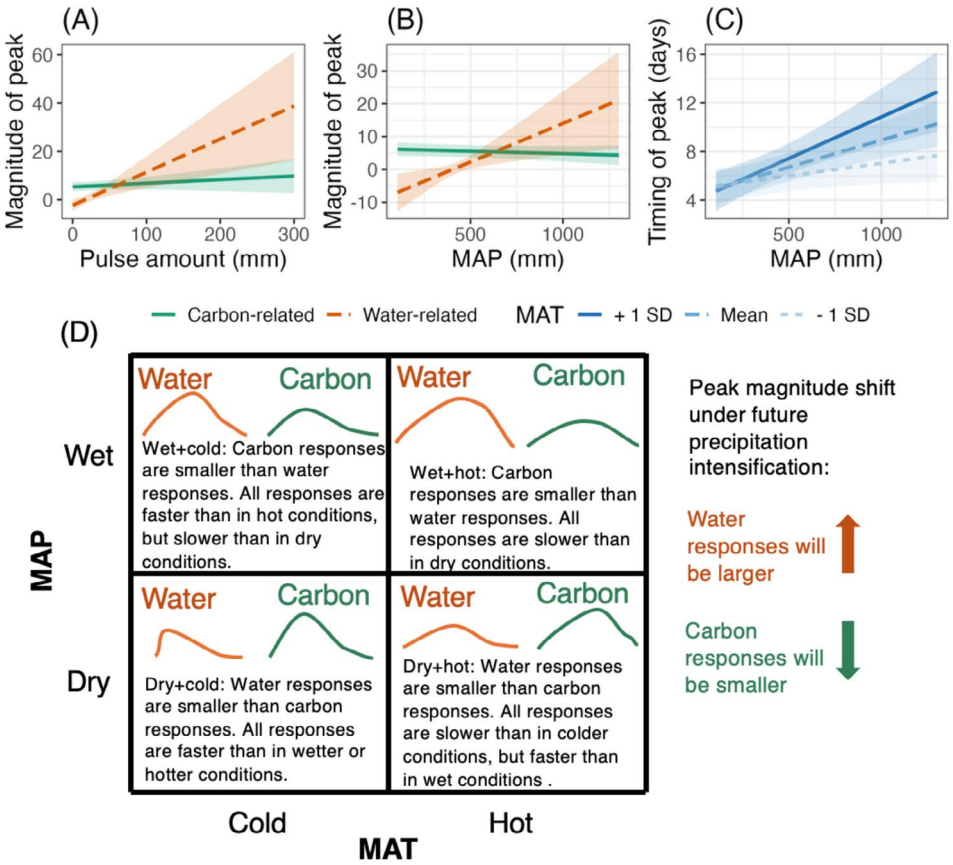


**FIGURE 6** | Predicted responses of carbon-related (solid green lines) and water-related (dash orange lines) responses to precipitation pulses with respect to the timing ($t_{peak}$) and the magnitude ($y_{peak}$) of the peak pulse response. Interaction plots show that carbon- and water-related variables exhibit different relationships between (A) $y_{peak}$ and pulse amount, with carbon-related variables responding more strongly to small pulses relative to water-related pulse responses, but relatively less to large pulses and (B) $y_{peak}$ and MAP, with carbon-related variables responding more strongly than water-related pulses in more arid (lower MAP) sites, but water-related responses responding more strongly than carbon-related responses in wetter sites. Across all response variables, interaction plots also show that (C) the relationship between $t_{peak}$ and MAP depends on MAT such that the timing of the peak response is more greatly delayed by MAP at hotter sites (higher MAT; thick blue lines) compared to cooler sites (lower MAT; light dashed blue). Shaded regions in (A)–(C) give the 95% CI interval. (D) Conceptual figure summarizing the interactions shown in (A)–(C) across the MAP-MAT plane for both carbon- and water-related responses; arrows to the right show the direction of potential future shifts in peak magnitude under each scenario if precipitation regimes become more intense.

difficulty in identifying such pulse dynamics or the expectation that they do not exist, despite evidence to the contrary (Feldman et al. 2021, 2024). Our synthesis indicates that it is valuable to understand pulse dynamics in less arid ecosystems, where dry-down periods are less pronounced and pulse experiments are less common, as precipitation pulses are also leading to substantial carbon- and water-related responses in these wetter systems.

Our results also indicate that the classic, hump-shaped pulse response (e.g., Noy-Meir 1973; Ogle and Reynolds 2004) is not ubiquitous. While this response shape is relatively common for soil respiration ($R_{bg}$; Figure 4A) and transpiration ($T$; Figure 4B), linear or muted hump-shaped (mixture of linear and Ricker) responses are also common across a wide array of plant and ecosystem response variables (Figure 4). The presence of some linear pulse responses could be the result of a short observation period, as it is possible that the response could have returned to near pre-pulse values if it was observed for a longer period (Vicca et al. 2012). On the other hand, if the affected organisms adjusted their physiology (acclimated) in response to a precipitation pulse (Niu et al. 2005; Schönbeck et al. 2022), we might expect that their associated response metric (e.g., $A_{net}$, $g_s$, $R_{eco}$) would not return to pre-pulse levels; thus, a linear or intermediate-shaped pulse response would be more likely in such cases. Regardless, our study shows that allowing for a wider range of pulse response shapes can better characterize pulse dynamics across a diversity of ecosystem types.

Importantly, we also found that precipitation pulse responses depend on spatial scale. We found that pulse responses were faster and had smaller peak magnitudes at large spatial scales, possibly because measurements at larger scales represent the aggregation of multiple processes. For example, ecosystem- or plot-scale net ecosystem exchange (NEE) is the result of leaf- and canopy-level photosynthesis and respiration, above- and belowground plant respiration, and belowground heterotrophic respiration, and each of these components may respond differently (Baldocchi et al. 2006; Williams et al. 2009) to a precipitation pulse, making the net response of NEE muted (or potentially exaggerated).

### 5.2 | Q2: When a Pulse Response Occurs, What Drives Its Timing, Magnitude, and Speed?

We expected that the pulse amount might partly govern the characteristics of the pulse response (e.g., Sponseller 2007; Heisler-White et al. 2008; Feldman et al. 2024). Although pulse amount did significantly interact with pulse response type, pulse amount was of little importance alone for the peak magnitude of the pulse response. This could be because the pulse responses are also being controlled by factors not captured here, such as phenology (Emmerich 2003). This would be consistent with past studies that found that rain-use efficiency converges on a maximum response (Huxman, Smith, et al. 2004) and that the relationship between primary production and precipitation amount is highly variable (le Houérou et al. 1988). Conversely, it is possible that response magnitude is strongly affected by situational environmental conditions not captured here, such as rainfall frequency (Manzoni et al. 2013; Holtzman et al. 2024) and antecedent moisture conditions, which may be more important than pulse amount for the magnitude of the pulse response (Chou et al. 2008; Cable et al. 2013; Barron-Gafford et al. 2014). At least in the case of dryland ecosystems that are likely adapted to infrequent, small precipitation events (Sala and Lauenroth 1982; Huxman, Smith, et al. 2004), it could be that a maximum response threshold is reached quickly, even in the case of small moisture pulse events. Unfortunately, we could not explicitly evaluate the role of precipitation frequency as this information was not frequently reported in the literature from which we extracted pulse response data (e.g., Vicca et al. 2012).

Regardless, small pulse amounts seem to stimulate larger responses of carbon-related compared to water-related response variables, but larger pulse amounts stimulate smaller responses of carbon-related compared to water-related response variables. This may mean carbon- and water-related responses could become more decoupled under less frequent but more intense precipitation regimes. However, this is dependent on ecosystem type, the extent to which precipitation pulse dynamics intensify, and the degree to which these changes shift carbon- and water-related responses. In particular, the timing and magnitude of the pulse response may vary across ecosystems differing in aridity and across different scales within an ecosystem (e.g., Figure 5, and Q3 below). For example, in drylands, where pulse responses peak faster after a precipitation pulse compared to more mesic environments, larger pulse amounts will likely more closely align the magnitude of water- and carbon-related responses. If pulse amounts exceed ~50 mm (Figure 6A) in drier ecosystems, carbon-related responses may have lower magnitude peaks than water-related responses. In wetter ecosystems, water-related responses already have larger peak magnitudes compared to carbon-related responses, so any increase in precipitation pulse amount would further decouple the timing of carbon- and water-related responses (Figure 6D).

Spatial scale also affected the speed of the pulse responses, since pulse responses were faster at larger spatial scales. This can be explained by the mixture of plant and soil processes when whole ecosystems are measured. For example, we might expect ET responses to occur more quickly than $g_s$ responses, because the physical process of evaporation—a component of ET—does not require biological upregulation to occur, as might occur for stomatal behavior.

### 5.3 | Q3: When a Pulse Response Occurs, How Does Site Aridity Affect the Pulse Response?

Plant and ecosystem responses to precipitation pulses clearly vary in relation to indices of aridity, and the relationship with aridity (e.g., MAP) differs between water- or carbon-related response variables. The pulse response behavior of water-related variables is more strongly influenced by aridity gradients compared to carbon-related responses (Figure 6B). At energy-limited sites that experience little water limitation (higher MAP), we could expect pulse responses to be longer and flatter since soil moisture would take longer to (and may never fully) deplete. We found this to be clearer for water-related responses compared to carbon-related responses at wet sites. At wet sites, carbon-related soil and ecosystem variables have slower responses to precipitation pulses than in dry conditions, perhaps due to soil microbial activity responding over longer periods (Matteucci et al. 2015), which would be magnified in wetter sites (higher MAP) that support higher microbial biomass (Collins et al. 2008; Evans et al. 2022). Moreover, we could expect plants in wetter sites to be less adapted to periods of water limitation, and energy-limited plants may have less capacity to quickly and efficiently respond to individual moisture inputs because their root zones are typically deeper (Scanlon and Goldsmith 1997; Seyfried et al. 2005), resulting in comparatively reduced access to immediate precipitation inputs. At the same time, pulse responses of energy-limited plants may have a more consistent signal over time as long as soil moisture is sufficiently available, which may be related to greater groundwater supply in mesic areas (Fan 2015; Fan et al. 2017; Feldman et al. 2024). Additionally, at sites with high MAP, soil-atmosphere water potential and vapor pressure gradients are generally weaker compared to more arid sites (Milly 1984; Saito et al. 2006), so any increase in soil moisture availability (e.g., due to a rain event) would likely lead to a less pronounced response in more mesic ecosystems. At water-limited sites, carbon-related variables showed higher magnitude responses to precipitation pulses compared to water-related responses, likely because the plant-governed water-related responses in drier ecosystems require an activation period (Kramer 1938; Gardner 1991; Collins et al. 2008). For example, following an extended dry period, precipitation events may trigger shallow root growth or foster tissue growth before a plant is able to fully capitalize on a precipitation event (Sala and Lauenroth 1982; Yan et al. 2000).

In general, drier sites were more likely to support fast pulse responses, and hot sites (regardless of average MAP) were more likely to exhibit greater magnitude (larger peaks) pulse responses. That is, site MAT and MAP appear to control the speed of a pulse response, but site MAT alone controls pulse response magnitude. The effects of MAP are also distinct between carbon- and water-related responses, and we could expect a range of distinct pulse response times under different combinations of MAP and MAT (Figure 6C,D).

## 6 | Methodological Advantages

Evaluating classic, hump-shaped pulse responses, as described in the pulse-reserve paradigm, is often the focus in studies aimed at understanding the effects of precipitation frequency and amount on plant and ecosystem behavior (e.g., Huxman, Snyder, et al. 2004; Ogle and Reynolds 2004; Schwinning and Sala 2004). However, linear and intermediate pulse response behaviors reflect different types of responses, which also aggregate to affect regional and global carbon and water cycles, and are still subject to change under varying precipitation regimes. Understanding whether or not a water pulse stimulates a response, and the "shape" of that response, is important to consider when comparing ecosystem functioning under different precipitation regimes across environmental gradients.

## 7 | Conclusion

Individual precipitation pulse events are foundational to understanding precipitation and drought impacts at longer timescales. From a meta-analysis of 587 pulse experiments conducted across 41 studies, we find that classical, hump-shaped pulse responses are the most commonly reported response shape, but other response shapes occur regularly and have different environmental impacts and may arise due to different mechanisms. The timing and magnitude of the peak response are interactively controlled by MAP, MAT, and whether a response is carbon- or water-related, such that water-related pulse responses are smaller and faster than carbon-related pulse responses at dry sites compared to wet sites. This framework for describing the controls on pulse dynamics can help anticipate the impacts of increased precipitation variability under climate change.

### Author Contributions

**Emma Reich:** data curation, formal analysis, methodology, visualization, writing – original draft, writing – review and editing. **Jessica Guo:** conceptualization, data curation, formal analysis, methodology, visualization, writing – original draft, writing – review and editing. **Drew Peltier:** data curation, writing – review and editing. **Emily Palmquist:** data curation, writing – review and editing. **Kimberly Samuels-Crow:** conceptualization, data curation, writing – review and editing. **Rohan Boone:** data curation. **Kiona Ogle:** conceptualization, formal analysis, methodology, visualization, writing – review and editing.

### Acknowledgments

We would like to thank Volodymyr Saruta and Abraham Cadmus for assistance with the data extraction. We acknowledge support from the US National Science Foundation (NSF-EAR-1834699). Any use of trade, firm, or product names is for descriptive purposes only and does not imply endorsement by the US Government.

### Conflicts of Interest

The authors declare no conflicts of interest.

### Data Availability Statement

The data and code that support the findings of this study are openly available in Zenodo at https://doi.org/10.5281/zenodo.13942718 and Github at https://github.com/Ogle-lab/Pulse-meta-analysis.

### References

Baldocchi, D., J. Tang, and L. Xu. 2006. "How Switches and Lags in Biophysical Regulators Affect Spatial-Temporal Variation of Soil Respiration in an Oak-Grass Savanna." *Journal of Geophysical Research: Biogeosciences* 111, no. G2: 2005JG000063.

Barron-Gafford, G. A., J. M. Cable, L. P. Bentley, et al. 2014. "Quantifying the Timescales Over Which Exogenous and Endogenous Conditions Affect Soil Respiration." *New Phytologist* 202: 442–454.

Bolker, B. M. 2008. *Ecological Models and Data in R. Page Ecological Models and Data in R*. Princeton University Press.

Brooks, S. P., and A. Gelman. 1998. "General Methods for Monitoring Convergence of Iterative Simulations." *Journal of Computational and Graphical Statistics* 7: 434–455.

Cable, J. M., K. Ogle, G. A. Barron-Gafford, et al. 2013. "Antecedent Conditions Influence Soil Respiration Differences in Shrub and Grass Patches." *Ecosystems* 16: 1230–1247.

Chou, W. W., W. L. Silver, R. D. Jackson, A. W. Thompson, and B. Allen-Diaz. 2008. "The Sensitivity of Annual Grassland Carbon Cycling to the Quantity and Timing of Rainfall." *Global Change Biology* 14: 1382–1394.

Collins, S. L., J. Belnap, N. B. Grimm, et al. 2014. "A Multiscale, Hierarchical Model of Pulse Dynamics in Arid-Land Ecosystems." *Annual Review of Ecology, Evolution, and Systematics* 45: 397–419.

Collins, S. L., R. L. Sinsabaugh, C. Crenshaw, et al. 2008. "Pulse Dynamics and Microbial Processes in Aridland Ecosystems." *Journal of Ecology* 96: 413–420.

Delgado-Balbuena, J., H. W. Loescher, C. A. Aguirre-Gutiérrez, et al. 2023. "Dynamics of Short-Term Ecosystem Carbon Fluxes Induced by Precipitation Events in a Semiarid Grassland." *Biogeosciences* 20: 2369–2385.

Doke, J. 2024. "GRABIT." MATLAB Central File Exchange.

Emmerich, W. E. 2003. "Carbon Dioxide Fluxes in a Semiarid Environment With High Carbonate Soils." *Agricultural and Forest Meteorology* 116: 91–102.

Evans, S. E., S. D. Allison, and C. V. Hawkes. 2022. "Microbes, Memory and Moisture: Predicting Microbial Moisture Responses and Their Impact on Carbon Cycling." *Functional Ecology* 36: 1430–1441.

Fan, Y. 2015. "Groundwater in the Earth's Critical Zone: Relevance to Large-Scale Patterns and Processes." *Water Resources Research* 51: 3052–3069.

Fan, Y., G. Miguez-Macho, E. G. Jobbágy, R. B. Jackson, and C. Otero-Casal. 2017. "Hydrologic Regulation of Plant Rooting Depth." *Proceedings of the National Academy of Sciences* 114: 10572–10577.

Feldman, A. F., A. Chulakadabba, D. J. Short Gianotti, and D. Entekhabi. 2021. "Landscape-Scale Plant Water Content and Carbon Flux Behavior Following Moisture Pulses: From Dryland to Mesic Environments." *Water Resources Research* 57: e2020WR027592.

Feldman, A. F., X. Feng, A. J. Felton, et al. 2024. "Plant Responses to Changing Rainfall Frequency and Intensity." *Nature Reviews Earth and Environment* 5: 1–294.

Fick, S. E., and R. J. Hijmans. 2017. "WorldClim 2: New 1-Km Spatial Resolution Climate Surfaces for Global Land Areas." *International Journal of Climatology* 37: 4302–4315.

Garcia-Pichel, F., and O. Sala. 2022. "Expanding the Pulse–Reserve Paradigm to Microorganisms on the Basis of Differential Reserve Management Strategies." *Bioscience* 72: 638–650.

Gardner, W. R. 1991. "Modeling Water Uptake by Roots." *Irrigation Science* 12: 109–114.

Gelman, A., and D. B. Rubin. 1992. "Inference From Iterative Simulation Using Multiple Sequences." *Statistical Science* 7: 457–472.

Giorgi, F., F. Raffaele, and E. Coppola. 2019. "The Response of Precipitation Characteristics to Global Warming From Climate Projections." *Earth System Dynamics* 10: 73–89.

Hedges, L. V., J. Gurevitch, and P. S. Curtis. 1999. "The Meta-Analysis of Response Ratios in Experimental Ecology." *Ecology* 80: 1150–1156.

Heisler-White, J. L., A. K. Knapp, and E. F. Kelly. 2008. "Increasing Precipitation Event Size Increases Aboveground Net Primary Productivity in a Semi-Arid Grassland." *Oecologia* 158: 129–140.

Holtzman, N., B. Sloan, A. Potkay, G. Katul, X. Feng, and A. G. Konings. 2024. "Ecosystem Water-Saving Timescale Varies Spatially With Typical Drydown Length." *AGU Advances* 5: e2023AV001113.

Huxman, T. E., M. D. Smith, P. A. Fay, et al. 2004. "Convergence Across Biomes to a Common Rain-Use Efficiency." *Nature* 429: 651–654.

Huxman, T. E., K. A. Snyder, D. Tissue, et al. 2004. "Precipitation Pulses and Carbon Fluxes in Semiarid and Arid Ecosystems." *Oecologia* 141: 254–268.

Jacobson, T. W. P., R. Seager, A. P. Williams, I. R. Simpson, K. A. McKinnon, and H. Liu. 2024. "An Unexpected Decline in Spring Atmospheric Humidity in the Interior Southwestern United States and Implications for Forest Fires." *Journal of Hydrometeorology* 25: 373–390.

Kannenberg, S. A., D. R. Bowling, and W. R. L. Anderegg. 2020. "Hot Moments in Ecosystem Fluxes: High GPP Anomalies Exert Outsized Influence on the Carbon Cycle and Are Differentially Driven by Moisture Availability Across Biomes." *Environmental Research Letters* 15: e054004.

Kellner, K., and M. Meredith. 2024. "jagsUI: A Wrapper Around 'rjags' to Streamline 'JAGS' Analyses."

Koppa, A., J. Keune, D. L. Schumacher, et al. 2024. "Dryland Self-Expansion Enabled by Land-Atmosphere Feedbacks." *Science* 385: 967–972.

Kramer, P. J. 1938. "Root Resistance as a Cause of the Absorption Lag." *American Journal of Botany* 25: 110–113.

le Houérou, H. N., R. L. Bingham, and W. Skerbek. 1988. "Relationship Between the Variability of Primary Production and the Variability of Annual Precipitation in World Arid Lands." *Journal of Arid Environments* 15: 1–18.

Long, J. A. 2021. "Interactions: Comprehensive, User-Friendly Toolkit for Probing Interactions."

López-Ballesteros, A., P. Serrano-Ortiz, E. P. Sánchez-Cañete, et al. 2016. "Enhancement of the Net $CO_2$ Release of a Semiarid Grassland in SE Spain by Rain Pulses." *Journal of Geophysical Research: Biogeosciences* 121: 52–66.

Manzoni, S., G. Vico, S. Palmroth, A. Porporato, and G. Katul. 2013. "Optimization of Stomatal Conductance for Maximum Carbon Gain Under Dynamic Soil Moisture." *Advances in Water Resources* 62: 90–105.

Matteucci, M., C. Gruening, I. Goded Ballarin, G. Seufert, and A. Cescatti. 2015. "Components, Drivers and Temporal Dynamics of Ecosystem Respiration in a Mediterranean Pine Forest." *Soil Biology and Biochemistry* 88: 224–235.

Milly, P. C. D. 1984. "A Simulation Analysis of Thermal Effects on Evaporation From Soil." *Water Resources Research* 20: 1087–1098.

Niu, S. L., G. M. Jiang, S. Q. Wan, M. Z. Liu, L. M. Gao, and Y. G. Li. 2005. "Ecophysiological Acclimation to Different Soil Moistures in Plants From a Semi-Arid Sandland." *Journal of Arid Environments* 63: 353–365.

Novick, K. A., D. L. Ficklin, P. C. Stoy, et al. 2016. "The Increasing Importance of Atmospheric Demand for Ecosystem Water and Carbon Fluxes." *Nature Climate Change* 6: 1023–1027.

Noy-Meir, I. 1973. "Desert Ecosystems: Environment and Producers." *Annual Review of Ecology and Systematics* 4: 25–51.

Ogle, K., Y. Liu, S. Vicca, and M. Bahn. 2021. "A Hierarchical, Multivariate Meta-Analysis Approach to Synthesising Global Change Experiments." *New Phytologist* 231: 2382–2394.

Ogle, K., and J. F. Reynolds. 2004. "Plant Responses to Precipitation in Desert Ecosystems: Integrating Functional Types, Pulses, Thresholds, and Delays." *Oecologia* 141: 282–294.

Pendergrass, A. G., and D. L. Hartmann. 2014. "Changes in the Distribution of Rain Frequency and Intensity in Response to Global Warming." *Journal of Climate* 27: 8372–8383.

Pendergrass, A. G., R. Knutti, F. Lehner, C. Deser, and B. M. Sanderson. 2017. "Precipitation Variability Increases in a Warmer Climate." *Scientific Reports* 7: 17966.

Plummer, M. 2003. "JAGS: A Program for Analysis of Bayesian Graphical Models Using Gibbs Sampling."

Poisot, T., R. Sachse, J. Ashander, and T. Galili. 2016. "digitize: Use Data From Published Plots in R."

R Core Team. 2020. *R: A Language and Environment for Statistical Computing*. R Foundation for Statistical Computing.

Reynolds, J. F., P. R. Kemp, K. Ogle, and R. J. Fernández. 2004. "Modifying the 'Pulse–Reserve' Paradigm for Deserts of North America: Precipitation Pulses, Soil Water, and Plant Responses." *Oecologia* 141: 194–210.

Ricklefs, R. E. 2008. *The Economy of Nature*. W.H. Freeman and Company.

Saito, H., J. Šimůnek, and B. P. Mohanty. 2006. "Numerical Analysis of Coupled Water, Vapor, and Heat Transport in the Vadose Zone." *Vadose Zone Journal* 5: 784–800.

Sala, O. E., and W. K. Lauenroth. 1982. "Small Rainfall Events: An Ecological Role in Semiarid Regions." *Oecologia* 53: 301–304.

Santos e Silva, C. M., B. G. Bezerra, K. R. Mendes, et al. 2024. "Rainfall and Rain Pulse Role on Energy, Water Vapor and $CO_2$ Exchanges in a Tropical Semiarid Environment." *Agricultural and Forest Meteorology* 345: 109829.

Scanlon, B. R., and R. S. Goldsmith. 1997. "Field Study of Spatial Variability in Unsaturated Flow Beneath and Adjacent to Playas." *Water Resources Research* 33: 2239–2252.

Schönbeck, L., C. Grossiord, A. Gessler, et al. 2022. "Photosynthetic Acclimation and Sensitivity to Short- and Long-Term Environmental Changes in a Drought-Prone Forest." *Journal of Experimental Botany* 73: 2576–2588.

Schwinning, S., and O. E. Sala. 2004. "Hierarchy of Responses to Resource Pulses in Arid and Semi-Arid Ecosystems." *Oecologia* 141: 211–220.

Scott, R. L., and J. A. Biederman. 2017. "Partitioning Evapotranspiration Using Long-Term Carbon Dioxide and Water Vapor Fluxes: New Approach to ET Partitioning." *Geophysical Research Letters* 44: 6833–6840.

Seyfried, M. S., S. Schwinning, M. A. Walvoord, et al. 2005. "Ecohydrological Control of Deep Drainage in Arid and Semiarid Regions." *Ecology* 86: 277–287.

Sponseller, R. A. 2007. "Precipitation Pulses and Soil $CO_2$ Flux in a Sonoran Desert Ecosystem." *Global Change Biology* 13: 426–436.

The MathWorks Inc. 2020. "MATLAB." Version: 9.8.0.1417392. Natick, Massachusetts.

Trenberth, K. E. 2011. "Changes in Precipitation With Climate Change." *Climate Research* 47: 123–138.

Vicca, S., A. K. Gilgen, M. Camino Serrano, et al. 2012. "Urgent Need for a Common Metric to Make Precipitation Manipulation Experiments Comparable." *New Phytologist* 195: 518–522.

Williams, A. P., B. I. Cook, and J. E. Smerdon. 2022. "Rapid Intensification of the Emerging Southwestern North American Megadrought in 2020–2021." *Nature Climate Change* 12: 232–234.

Williams, C. A., N. Hanan, R. J. Scholes, and W. Kutsch. 2009. "Complexity in Water and Carbon Dioxide Fluxes Following Rain Pulses in an African Savanna." *Oecologia* 161: 469–480.

Wohlfahrt, G., L. F. Fenstermaker, and J. A. Arnone III. 2008. "Large Annual Net Ecosystem $CO_2$ Uptake of a Mojave Desert Ecosystem." *Global Change Biology* 14: 1475–1487.

Yan, S., C. Wan, R. E. Sosebee, D. B. Wester, E. B. Fish, and R. E. Zartman. 2000. "Responses of Photosynthesis and Water Relations to Rainfall in the Desert Shrub Creosote Bush (*Larrea tridentata*) as Influenced by Municipal Biosolids." *Journal of Arid Environments* 46: 397–412.

**Supporting Information**

Additional supporting information can be found online in the Supporting Information section.